

Deep Space Optical Communications Link Availability and Data Volume

A. Biswas, K. E. Wilson, S. Piazzolla, J. Wu, W. H. Farr

*Jet Propulsion Laboratory, California Institute of Technology
4800 Oak Grove Drive, Pasadena, CA 91109*

ABSTRACT

Optical links from a spacecraft at planetary distance to a ground-based receiver presume a cloud free line of site (CFLOS). Future ground-based optical receiving networks, should they be implemented, will rely on site diversity of cloud cover to increase link availability. Recent analysis shows that at least 90% and as high as 96% CFLOS availability can be realized from a cluster comprised of 3-4 nodes. During CFLOS availability variations of atmospheric parameters such as attenuation, sky radiance and “seeing” will determine the link performance. However, it is the statistical distributions of these parameters at any given node that will ultimately determine the data volumes that can be realized. This involves a complex interaction of site-specific atmospheric parameters. In the present work a simplified approach toward addressing this problem is presented. The worst-case link conditions for a spacecraft orbiting Mars, namely, maximum range (2.38 AU) and minimum sun-Earth-probe (SEP) angle of 3-10° is considered. A lower bound of ~100 Gbits/day under the most stressing link conditions is estimated possible.

1. INTRODUCTION

The Mars Laser Communications Demonstration (MLCD) Project^{1,2,3} initiated by NASA has stimulated renewed interest in deep space optical communications, with an emphasis on optical links from Mars. In this article link availability and data volumes from Mars to a ground-based optical network are discussed. MLCD link characteristics are used in presenting the discussion.

The eventual implementation of an Earth optical receiving network for providing data service to NASA’s planetary spacecraft will be the subject of much future study. The available options are space, high altitude platforms (for example, balloons) or ground. Space-based reception of laser communications transmitted from deep-space, completely bypasses ground-based network disadvantages associated with cloud cover and atmospheric turbulence. Putting receivers on balloons or other suitable high altitude platforms completely eliminates cloud blockage and largely mitigates atmospheric effects. It is the relatively lower cost of ground-based networks that makes them worth considering, at least in the near term. The critical question for a ground-based network is: the quality of data service firstly, due to cloud blockage and secondly, by atmospheric degradation, even when a cloud-free line-of-sight (CFLOS) between spacecraft and ground-station is available? Once this question is satisfactorily answered the performance penalty by virtue of being on the ground can be compared to the perceived cost saving.

A future optical ground-based network would be comprised of nodes carefully selected for the prevalence of clear cloud free skies, as well as, low atmospheric attenuation, sky brightness and good atmospheric “seeing”. Cloud cover statistics for selected nodes of the network can be utilized to determine an overall CFLOS availability. During CFLOS the large variability of the atmospheric parameters will influence link performance and therefore data volumes. Conceptually the most effective ground networks will not only provide the maximum CFLOS but also be comprised of nodes that provide a high percentage of relatively benign atmospheric conditions. Additionally, ground station design will determine minimum operational Sun-Earth-probe (SEP) angles that affect link availability. For example, for a spacecraft orbiting Mars the outage during solar conjunction can be limited to 3% of a Martian year by designing a ground station that can operate while pointing within 3-degrees of the sun. Finally, predictive capability coupled with an effective handover strategy, given the long light times, is critical to achieving optimal operations with a ground-network. In this article the predictive models for weather and atmospheric conditions will not be addressed, instead atmospheric channel statistics will be cited to present some preliminary discussions about link availability and data volumes.

As elaborated below the data needed to comprehensively address all of the above considerations is incomplete. However, some lower bounds can be predicted based upon the limited data that is available and discussed below. Existing astronomical observatory sites share many of the attributes desired for deep-space optical receiving ground stations, with the additional requirement of operating not only in the daytime but at very small Sun separation angles.

Finally, the data rates used to estimate data volumes utilize the Mars Laser Terminal (MLT) transmission characteristics, namely, a 5 W average power laser transmitted by a 30-cm diameter diffraction limited telescope. Furthermore, 5-m diameter telescopes similar to the Hale telescope at Palomar Mountain are assumed for reception of the downlink at 1064-nm. Single photon-counting detectors with 30% photo-detection efficiency are assumed for the optical receivers.

2. GROUND NETWORK CONFIGURATION AND CLOUD STATISTICS

Ground network configurations for receiving deep space optical communications have been conceptualized for a while⁴. Some of the popular configurations described have been a linearly dispersed optical subnet (LDOS) and a clustered optical subnet COS. These are represented in Figure 1 by stars and circles respectively.

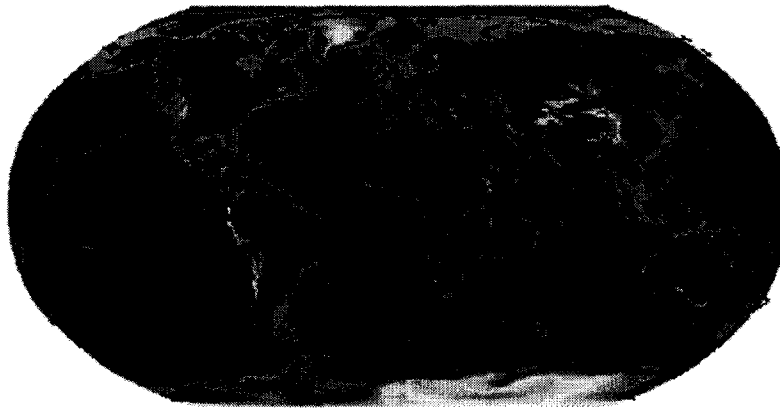


Figure 1 Two alternate configurations for globally distributing optical receivers represented by stars, linearly dispersed optical subnet (LDOS) and circles, clustered optical subnet (COS)

The global distribution is configured to maintain line-of-sight (LOS) with planetary spacecraft as the Earth rotates. Furthermore, the ability to “switch” the link to an alternate site as a work around against cloud blockage is intended. Ideally the nodes in either of the two configurations shown should be anti-correlated in weather.

Studies based upon many years of National Climate Data Center surface observations⁵ of cloud cover were analyzed for sites scattered over the South Western United States of America and generally availability could be enhanced from 60-70% for a single site to 80-95% to the combination of three sites.

More recently a study of cloud cover⁶ was undertaken utilizing satellite imagery. The spatio-temporal resolution of this approach is determined by the pixel angular field-of-view and the frequency at which images are acquired. The spatial resolution is 5km and the temporal resolution is one hour. CFLOS availability of sites predominantly in the South Western continental United States (CONUS) and Hawaii was determined. Various combinations of these sites were then analyzed to determine the overall CFLOS availability of a ground-based optical receiving network with a spacecraft assumed to be in Mars orbit. The details of this study are reported elsewhere⁶. Figure 2 summarizes the findings for a combination of a four site cluster comprised of Goldstone, CA, Kitt Peak, AZ, McDonald Observatory, TX and Mauna Kea, Hawaii where the CFLOS availability is presented by quarter. The overall CFLOS availability of this hypothetical network is 90%. With the year 1998 being an exception most likely associated with El Nino, the first quarter of the other years display relatively lower availability. This is attributed to both the Northern hemisphere winter

and declination of a Mars orbit causing the spacecraft not rise very high in the sky and resulting in a relatively shorter pass. Therefore, re-configuring the cluster to include a node in the S. Hemisphere should enhance the availability. Unfortunately this cannot be verified in a statistically significant way because the data were not available. However, based on 6-months of data it was verified that a 3-site cluster comprised of Kitt Peak, AZ, Haleakala, HI and Paranal Chile an overall availability of 96% was possible with the minimum availability being 90%. To summarize the cloud statistical study indicates that at least overall 90% availability has been shown by analyzing 6-years of data while an improved availability of 96% with a minimum of 90% seems feasible though further long term data analysis is required to verify this.

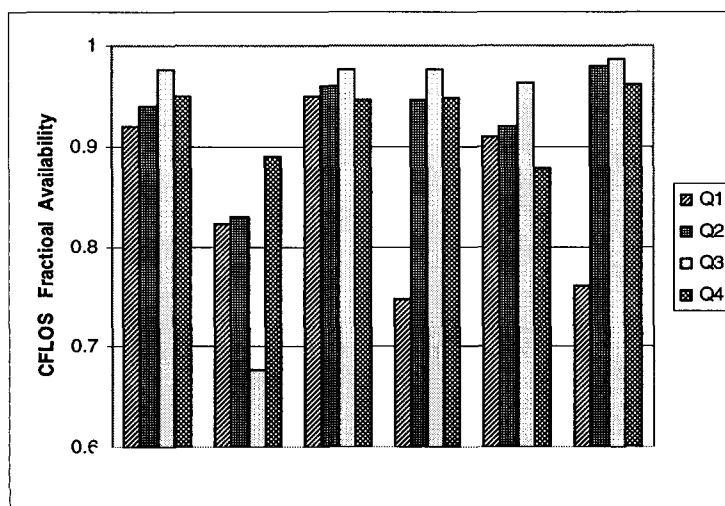


Figure 2 Summary of CFLOS availability for a 4-site cluster comprised of Goldstone, CA, Kitt Peak, AZ, McDonald Observatory, TX and Mauna Kea, Hawaii shown by quarter for 6-years.

3. PERFORMANCE DURING CFLOS

Given the foregoing discussion the performance of a single network node during CFLOS availability is addressed next. Other outages associated with ground network nodes have to do with the configuration with respect to the planets and the sun. Therefore as pointed out earlier, for a spacecraft orbiting Mars, an outage of 3% of the Martian year is introduced due to the inability of the space and ground terminals to “stare” at the sun. An additional 2% outage is associated with eclipsing of the spacecraft by the planet Mars though this is not unique to optical communications.

Besides cloud blockage and the other less significant outages above, performance of a ground station is related to the variability of atmospheric conditions. Attenuation, sky radiance and atmospheric “seeing” are the key parameters that display seasonal as well as diurnal variations. The MLC D Project will provide a good opportunity for evaluating the impact of atmospheric variability on link performance. The discussion that follows makes predictions based on limited data and its statistical variations.

3.1 Atmospheric Attenuation

Atmospheric modeling tools such as MODTRAN⁷ can predict attenuation for a variety of assumed aerosol profiles. A good example of this is depicted in Figure 3 where three different atmospheric aerosol models, namely, desert extinction with 12 m/s wind speed, rural aerosol with 23-Km visibility and rural aerosol with 5-Km visibility. Moreover the attenuation is shown for zenith angles of 0 and 70 degrees. Assuming a ground station maximum viewing zenith angle is 70 degrees as the spacecraft rises the attenuation will decrease until the spacecraft rises to its maximum zenith angle and then will start increasing again. In order to assess link availability knowledge of the statistical fluctuations of attenuation are desired. Models for predicting attenuation do not reveal the statistical distributions of attenuation for a

particular site. Furthermore the cloud cover statistics for a particular site can be influenced by local or regional wind patterns, topology and geography.

Spectral attenuation of the atmosphere is being measured at Table Mountain, CA and Mount Lemmon, Arizona using star light transmission with the Atmospheric Visibility Monitoring⁸ (AVM) stations. Figure 4 shows a typical quarterly cumulative distribution function for atmospheric attenuation at the zenith.

The AVM stations use a thermoelectrically cooled, commercially available, back-thinned charge coupled device (CCD), sensor for recording star images. Consequently the sensitivity at 1064-nm in the presence of daytime backgrounds is poor and reliable statistics cannot be gathered. Therefore the data at 1064-nm represents pre-dominantly nighttime attenuation statistics whereas the 860-nm is representative of both daytime and nighttime statistics. Table 1 shows spectral zenith attenuation in dB as a function of percentage cumulative probabilities. The data is predominantly from Table Mountain, CA with one quarter of Mount Lemmon data. The blanks in the Table 1 indicate that no data was

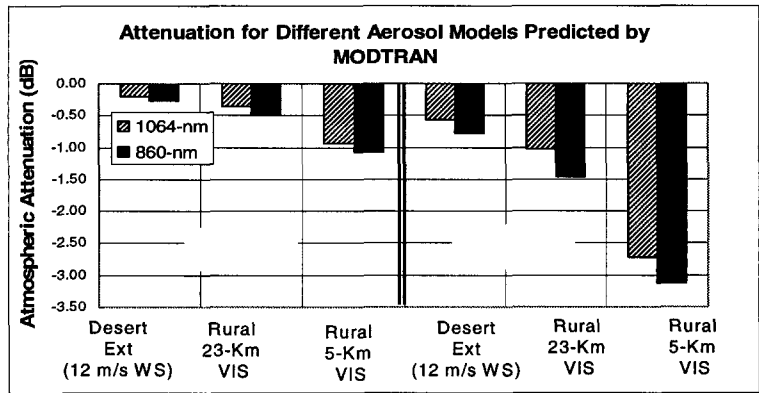


Figure 3 Atmospheric attenuation at 860- and 1064-nm predicted by MODTRAN for Desert Extinction with 12 m/s wind speed, Rural aerosols with 23-Km visibility and rural visibility with 5-Km visibility for two zenith angles of 0 and 70°

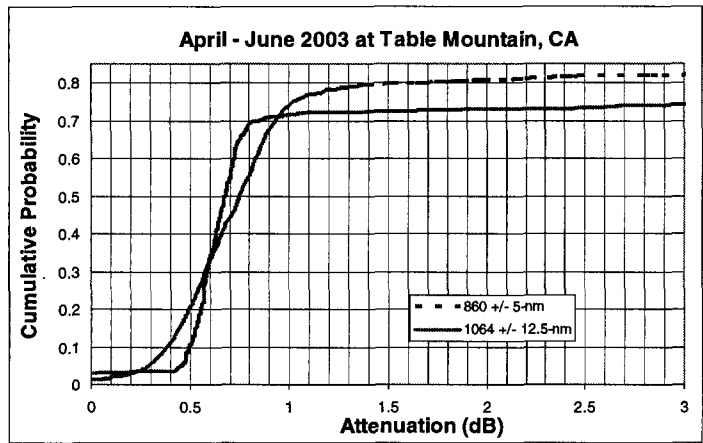


Figure 4 Typical cumulative distribution functions for atmospheric attenuation measured with the AVM station at Table Mountain, CA during the second quarter of 2003

acquired. If the simple assumption is made that ~3-dB or larger attenuation represents a link outage then the overall availability from the viewpoint of spectra attenuation will be 70-80%. This is consistent with the 6-year cloud cover study report⁶ where 80% was reported for the single site availability for Table Mountain, CA. Moreover Table 1 shows that in the winter quarter the attenuation can reduce single site availability to 40-50%. For

the winter quarter of 2003 Mount Lemmon shows an overall lower attenuation compared to Table Mountain at 860-nm.

If Table Mountain were a node of a ground-based network then other nodes would have to be relied upon to provide the overall 90-95% availability discussed earlier. For durations when links can be established the zenith attenuation will vary from less than 0.5 dB (about 10% or less time) to 1-1.5 dB (70-80% of the time) with some exceptions when the upper availability percentages could dip down to 50-60%.

Table 1 Summary of the percentage cumulative probability of measuring spectral attenuation in dB, at 1064- and 860-nm for a 2002 and 2003 from Table Mountain, CA

1064-nm with 25-nm bandpass						
Location	Quarter	Station Uptime Fraction	<2-dB	<1.5-dB	<1-dB	<0.5 d-B
TMF	Q3, 2002	0.33	0.8	0.79	0.73	0.15
TMF	Q4, 2002	0.62	0.62	0.6	0.56	0.45
TMF	Q1, 2003	0.85				
ML	Q1, 2003	0.4	0.62	0.58	0.5	0.2
TMF	Q2, 2003	0.85	0.73	0.73	0.7	0.4
TMF	Q3, 2003	0.7	0.68	0.65	0.53	0.4
860-nm with 10-nm bandpass						
Location	Quarter	Station Uptime Fraction	<2-dB	<1.5-dB	<1-dB	<0.5 d-B
TMF	Q3, 2002	0.33	0.87	0.83	0.78	0.35
TMF	Q4, 2002	0.62	0.65	0.62	0.58	0.35
TMF	Q1, 2003	0.85	0.4	0.35	0.25	0.05
ML	Q1, 2003	0.4	0.5	0.46	0.45	0.27
TMF	Q2, 2003	0.85	0.83	0.8	0.75	0.4
TMF	Q3, 2003	0.7	0.81	0.72	0.53	0.2

3.1 Sky Radiance

During daytime optical links that prevail two-thirds of the time when communicating with a spacecraft in Mars orbit sky radiance is the dominant source of background. Even though narrow band-pass filters and polarization discrimination together with properly designed stops and baffles will be used a significant amount of in-band background will influence link performance. Predicting the bounds of sky radiance can be achieved by the use of models and once again site-specific measurements provide sky radiance distributions that can then be used to assess link performance over time.

Figure 5 shows sky radiance predicted under assumptions identical to those used for attenuation in Figure 3 superimposed on measurements made at Table Mountain, CA. The measurements were made using a CIMEL Instrument used by the Aerosol Robotic Network⁹ (AERONET). The measurements depicted in Figure 5 are the raw sky radiance measurements and have not been filtered for cloud cover. Therefore some of the higher measurements may not be relevant to optical communications. The measurements represent variation of sky radiance with sun separation angle for observations made at sun zenith angle of 50-55 degrees. The peak shown on the theoretical predictions is an artifact because MODTRAN actually generates a singularity at 0 degrees sun separation. Generally speaking the model predictions are validated by the measurements.

Figure 6 shows a cumulative distribution function of sky radiance measured at Table Mountain, CA. The distributions represent data acquired during two campaigns during January-February 2000 and June 2003 – January

2004. Measurements were made at sun separation angles of 3-degrees and combine data acquired along the principle plane and in almucantar. The dependence on the location of the sun in the sky is also shown. The fact that on both occasions the sky radiance was larger at lower sun zenith angles is not understood, because models would suggest higher values of sky radiance at larger zenith angles due to the greater air-mass and scattering volume. This anomaly was not observed from a few other AERONET sites investigated.

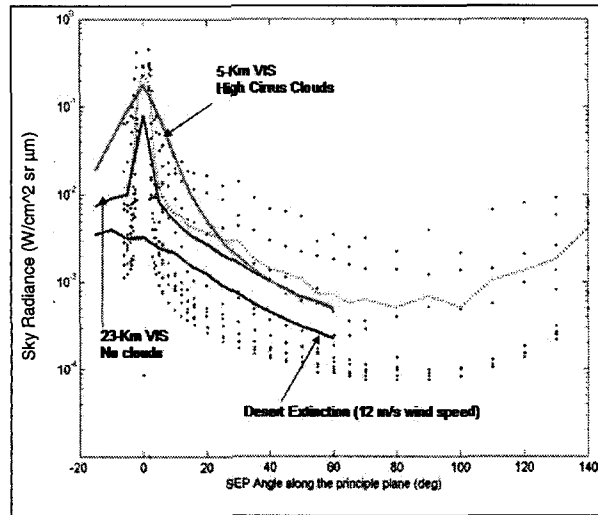


Figure 5 Sky radiance predicted by MODTRAN (solid lines) superimposed on measurements made during January-February, 2000 at Table Mountain, CA. The dotted line represents the average of measured sky radiance measurements made at sun zenith angles of 50-55 degrees

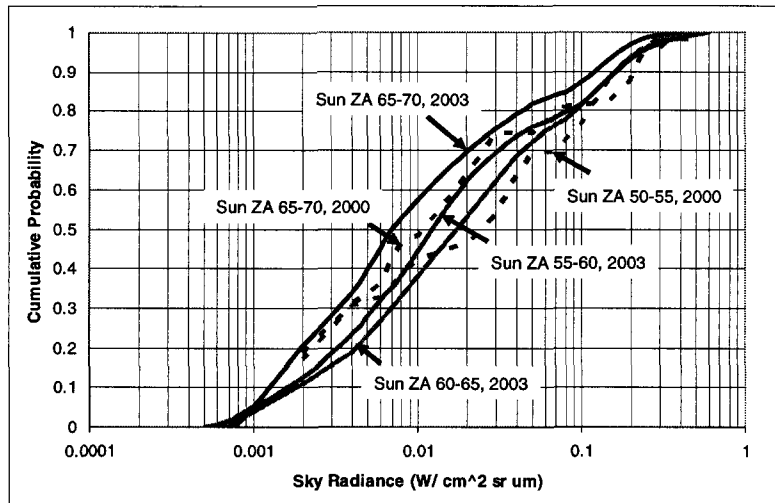


Figure 6 Cumulative probability distribution of sky radiance measured at Table Mountain, CA during January-February, 2000 and June 2003 to January 2004. Measurements were made at a sun separation of 3-degrees both along the principle plane and in almucantar

3.3 Atmospheric Seeing

Atmospheric “seeing” determines the blurring of the spot at the focal plane^{10,11} of a receiving optical system. In other words the solid angle of sky imaged in order to collect the laser signal is determined by prevalent atmospheric “seeing” related to the atmospheric coherence diameter (Fried parameter, r_0). Therefore combined with sky radiance distribution, the prevalent r_0 or “seeing” will determine the additive background light experienced by an

optical link. Though examples of long daytime seeing statistics exist, it is the simultaneous sky radiance and “seeing” data that is of interest. At the time of this report such data was not available.

4. AVAILABILITY AND DATA VOLUME

The foregoing discussion should make it apparent that predicting data volumes for a global optical receiving network is complex problem since statistically significant distributions of a number of site-specific atmospheric parameters in addition to cloud-blockage statistics is needed. Addressing this is beyond the scope of the present report.

A simplified analysis intended to identify a lower bound of data volume, under worst case link conditions (maximum range and minimum SEP angles of 3-10°) for a Mars orbiting spacecraft, communicating to a ground based network will be considered. In order to do so we fix “seeing” to be 10-cm and 6.8-cm at 55° and 70° zenith angles. These zenith angles were chosen based on the assumption that the ground station cannot look beyond 70° due to local topology and tree-line whereas the spacecraft does not rise over 55° during the solar conjunction of 2010-2011 (MTO mission) for a South Western US ground site. Utilizing the distribution of sky radiance and the fixed r_0 , as well as, accounting for the atmospheric attenuation distributions discussed the average background light and signal photons are plotted as diamonds in Figure 7. The background estimates include a fixed allocation of 0.01 photons/ns contributed by sunlight reflected from Mars and 0.03 photons/ns of stray light. For comparison the squares and triangles show the increase in signal and reduction in background as range decreases and SEP angle increases.

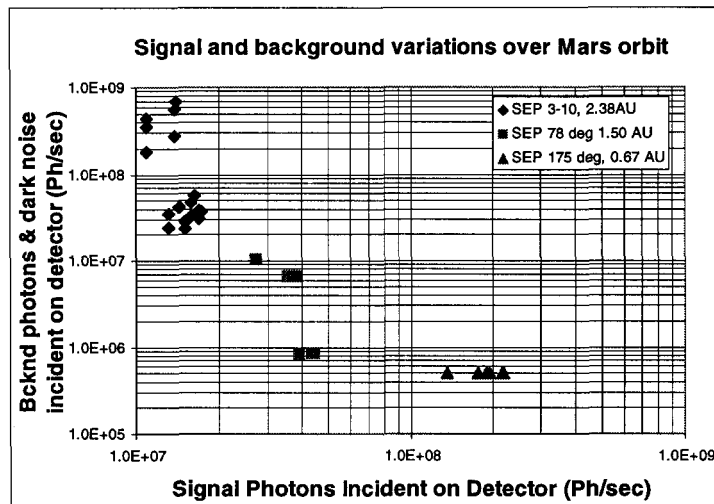


Figure 7 Distribution of signal and background during a single Mars orbit. The statistical variation of sky radiance and atmospheric attenuation for fixed “seeing” was accounted for during maximum range (2.38 AU) and 3-10 degree SEP angle (diamonds). The other data at 1.5 and 0.67 AU are nominal and included for reference

Thus between daytime sky with SEP angles ranging from 3-10° (2.38 AU) to 78° (1.5 AU) to nighttime sky SEP angle 175° (0.67 AU) three decades of background light and 1 decade of signal variation are apparent. Note that this combination of signal and background was obtained for the MLT parameters and a 5-m diameter aperture telescope similar to the Hale Telescope on the ground. The laser transmitter had nominally 5-W average power and was limited to a peak power of 300 W. A pulse-position modulation (PPM) is assumed with the maximum alphabet size of 64, consistent with the laser peak power. Moreover, the statistical sky radiance and atmospheric attenuation is representative of values measured at Table Mountain, CA.

The signal and background are incident upon photon-counting detector with 30% detection efficiency and 10000 counts per second of dark noise. Furthermore a 1-dB receiver implementation loss and a 0.75-dB gap from theoretical channel capacity¹² were assumed in order to evaluate the data rates.

The data rates along with code rates were evaluated both with and without 3-dB link margin. The code rates were forced to be close to 0.5 by varying the PPM slot width. Some of these results are shown in Figure 8. The filled and empty squares represent the data rates achievable during maximum range and 3-10° SEP angles. The empty squares indicate between 2-3 Mbps 20-50% of the time with 3-dB margin. The filled squares indicate between 1-2 Mbps 50-85% of the time but in this case there is no margin. In other words if the link were designed for 20-50% of the CFLOS availability with 3-dB margin the increase in background the other 35% of the time would still allow closing the link but the margin would be depleted. The remaining 15% of the time some data rates less than 1Mbps would be realized. Note that in order to keep code rate close to 0.5 the PPM slot width is 20-30-ns for the 2-3 Mbps and 30-40-ns for 1-2 Mbps. Also shown by diamonds and triangles are nominal data rates corresponding to 4-ns slot widths that would be achievable at other times during the mission.

Based on the foregoing a rather simple estimate of the lower bound of data volume can be made. Let us assume that all the clusters and nodes of the network performed on an average like the hypothetical site analyzed. Assume the network is made up of three clusters distributed around the globe. Depending on the distribution of nodes in a given cluster 90-95% availability is possible. In our lower bound estimate 90% is assumed. This means that for this operational network 90% of a 24-hour day CFLOS is available. Outages due to eclipsing of the spacecraft by the planet are neglected. Of the CFLOS availability the 15% estimate when the link operates at less than 1 Mbps is taken an outage in other words only 85% of the CFLOS availability is assumed to contribute to data volumes. Of this 85% we assume 2 Mbps 50% of the time and 1 Mbps 35% of the time. Therefore in a 24-hour day about 104 Gigabits/day of data can be received.

A conservative lower bound estimate of data volume under the most stressing atmospheric conditions for a Mars orbiting spacecraft is attempted here. Furthermore this analysis applies to the use of 5-m, rather than 10-m diameter receiver apertures. The worst case “seeing” will not prevail all of the time and the lower bounds of the possible data rates were used in computing the data volumes.

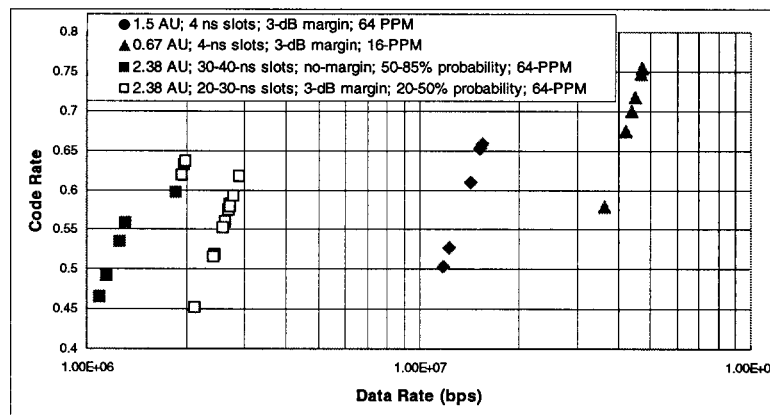


Figure 8 Representative data rates corresponding to the signal and background light combinations shown in Fig 7.

ACKNOWLEDGEMENTS

The authors would like to thank Mark Helmlinger for help in providing the AERONET sky radiance data and Mitchell Troy for providing valuable insights on atmospheric seeing at Palomar Mountain. The Jet Propulsion Laboratory, California Institute of Technology carried out the research described in this paper, under contract with the National Aeronautics and Space Administration

REFERENCES

1. B. L. Edwards, et al. "Overview of the Mars Laser Communications Demonstration Project," *AIAA Space 2003 Conference*, Paper 2003-6417
2. D. Boroson, A. Biswas, B. L. Edwards, "MLCD: Overview of NASA's Mars Laser Communications Demonstration System," *SPIE Proceedings, Vol. 5338: Free Space Laser Communications Technologies XVI*, [Ed. S. Mecherle], January 27, 2004
3. D. Boroson, R. S. Bondurant and J. J. Scozzafava, "Overview of High Rate Deep Space Laser Communications Options," *SPIE Proceedings, Vol. 5338: Free Space Laser Communications Technologies XVI*, [Ed. S. Mecherle], January 27, 2004
4. K. Shaik et al., "Ground Based Advanced Technology Study (GBATS); Optical Subnet Concepts for the DSN," Jet Propulsion Laboratory, D-11000, Release I, August 5, 1994.
5. S. Piazzolla and S. Slobin, "Statistics of Link Blockage Due to Cloud Cover for Free-Space Optical Communication Using NCDC Surface Weather Observation Data," *SPIE Proceedings, Volume 4635, Free Space Laser Communications Technologies XIV*, [Ed. S. Mecherle], 138, 2002.
6. M.E. Craddock, R. J. Allis, R. P. Link, S. Applegate, K. G. Davison, K. E. Wilson, "Mitigating the Effects of Clouds On Optical Communications," *SPIE Proceedings, Volume 5338B: Free-Space Laser Communication Technologies XVI*, January 29, 2004 *SPIE Proceedings, Volume 5338B: Free-Space Laser Communication Technologies XVI* [Ed. S. Mecherle], January 29, 2004
7. A. Berk, L.S. Bernstein, and D.C. Robertson, "MODTRAN: A Moderate Resolution Model for LOWTRAN 7," Air Force Geophysics Laboratory Technical Report GL-TR-89-0122, Hanscom AFB, MA.
8. B. Sani, A. Datta, D. Tsiang, J. Wu and A. Biswas, "Preliminary Results of an Upgraded Atmospheric Visibility Monitoring Station," *JPL TMO Progress Report*, 42-142, 2000.
9. <http://aeronet.gsfc.nasa.gov>
10. F. I. Khatri, D. M. Boroson, D. V. Murphy and J. Sharma, "Link Analysis of Mars-Earth Optical Communications System," *SPIE Proceedings, Volume 5338A, Free Space Laser Communications Technologies XVI*, [Ed. S. Mecherle], January 27, 2004.
11. A. Biswas and S. Piazzolla, "Deep-space Optical Communications Downlink Budget from Mars: System Parameters," *IPN Progress Report*, 42-154, Jet Propulsion Laboratory, Pasadena, CA, August 15, 2003.
12. B. Moision and J. Hamkins, "Deep-Space Optical Communications Downlink Budget: Modulation and Coding," *IPN Progress Report*, 42-154, Jet Propulsion Laboratory, Pasadena, CA, August 15, 2003.